Published online 4 October 2006 *Nucleic Acids Research, 2006, Vol. 34, No. 19* ***5449–5460***
doi:10.1093/nar/gkl596

Quantitative analysis of the oxidative DNA lesion, 2,2-diamino-4-(2-deoxy-β-D-*erythro*-pentofuranosyl)amino]-5(2*H*)-oxazolone (oxazolone), *in vitro* and *in vivo* by isotope dilution-capillary HPLC-ESI-MS/MS

Brock Matter, Danuta Malejka-Giganti[1,2], A. Saari Csallany[3] and Natalia Tretyakova*

Department of Medicinal Chemistry, University of Minnesota Cancer Center, University of Minnesota, Minneapolis, MN 55455, USA, [1]Veterans Affairs Medical Center, Minneapolis, MN 55417, USA, [2]Department of Laboratory Medicine and Pathology, University of Minnesota, Minneapolis, MN 55455, USA and [3]Department of Food Science and Nutrition, University of Minnesota, St Paul, MN 55108, USA

Received April 12, 2006; Revised July 7, 2006; Accepted August 1, 2006

ABSTRACT

A major DNA oxidation product, 2,2-diamino-4-[(2-deoxy-β-D-*erythro*-pentofuranosyl)amino]-5(2*H*)-oxazolone (oxazolone), can be generated either directly by oxidation of dG or as a secondary oxidation product with an intermediate of 8-oxo-7,8-dihydro-2′-deoxyguanosine (8-oxo-dG). Site-specific mutagenesis studies indicate that oxazolone is a strongly mispairing lesion, inducing ∼10-fold more mutations than 8-oxo-dG. While 8-oxo-dG undergoes facile further oxidation, oxazolone appears to be a stable final product of guanine oxidation, and, if formed *in vivo*, can potentially serve as a biomarker of DNA damage induced by oxidative stress. In this study, capillary liquid chromatography-electrospray ionization tandem mass spectrometry (HPLC-ESI-MS/MS) methods were developed to enable quantitative analysis of both 8-oxo-dG and oxazolone in DNA from biological sources. Sensitive and specific detection of 8-oxo-dG and oxazolone in enzymatic DNA hydrolysates was achieved by isotope dilution with the corresponding ^{15}N-labeled internal standards. Both nucleobase adducts were formed in a dose-dependent manner in calf thymus DNA subjected to photooxidation in the presence of riboflavin. While the amounts of oxazolone continued to increase with the duration of irradiation, those of 8-oxo-dG reached a maximum at 20 min, suggesting that 8-oxo-dG is converted to secondary oxidation products. Both lesions were found in rat liver DNA isolated under carefully monitored conditions to minimize artifactual oxidation. Liver DNA of diabetic and control rats maintained on a diet high in animal fat contained 2–6 molecules of oxazolone per 10^7 guanines, while 8-oxo-dG amounts in the same samples were between 3 and 8 adducts per 10^6 guanines. The formation of oxazolone lesions in rat liver DNA, their relative stability in the presence of oxidants and their potent mispairing characteristics suggest that oxazolone may play a role in oxidative stress-mediated mutagenesis.

INTRODUCTION

Reactive oxygen and nitrogen species, e.g. hydrogen peroxide, hydroxyl radical, superoxide, peroxynitrite and singlet oxygen, are produced in normal tissues as a result of aerobic metabolism, immune response and inflammation (1,2). The oxidative degradation of DNA has been implicated in aging, cancer and in some degenerative diseases (3–6). For example, smokers who exhibit low levels of hOgg1, a repair protein responsible for the removal of oxidative DNA lesions, are at an increased risk of lung cancer (7). Among the four DNA bases, guanine is most susceptible to oxidation because it has the lowest oxidation potential (8,9). Guanine oxidation is further facilitated in the GG and GGG repeats (8,10–12). Guanine oxidation gives rise to a variety of products, including 8-oxo-dG, spiroiminodihydantoin, guanidinohydantoin, 2-amino-5-[2-deoxy-β-D-*erythro*-pentofuranosyl)amino]-4*H*-imidazol-4-one (imidazolone) and its hydrolysis product, 2,2-diamino-4-[(2-deoxy-β-D-*erythro*-pentofuranosyl)amino]-5(2*H*)-oxazolone (oxazolone) (Scheme 1) (13–19).

Oxidized DNA nucleobases measured in target tissues can serve as biomarkers of oxidative stress and potentially,

*To whom correspondence should be addressed at 760E CCRB, University of Minnesota Cancer Center, 420 Delaware St SE, Mayo Mail Code 806, Minneapolis, MN 55455, USA; Tel: +1 612 626 3432; Fax +1 612 626 5135; Email: trety001@umn.edu

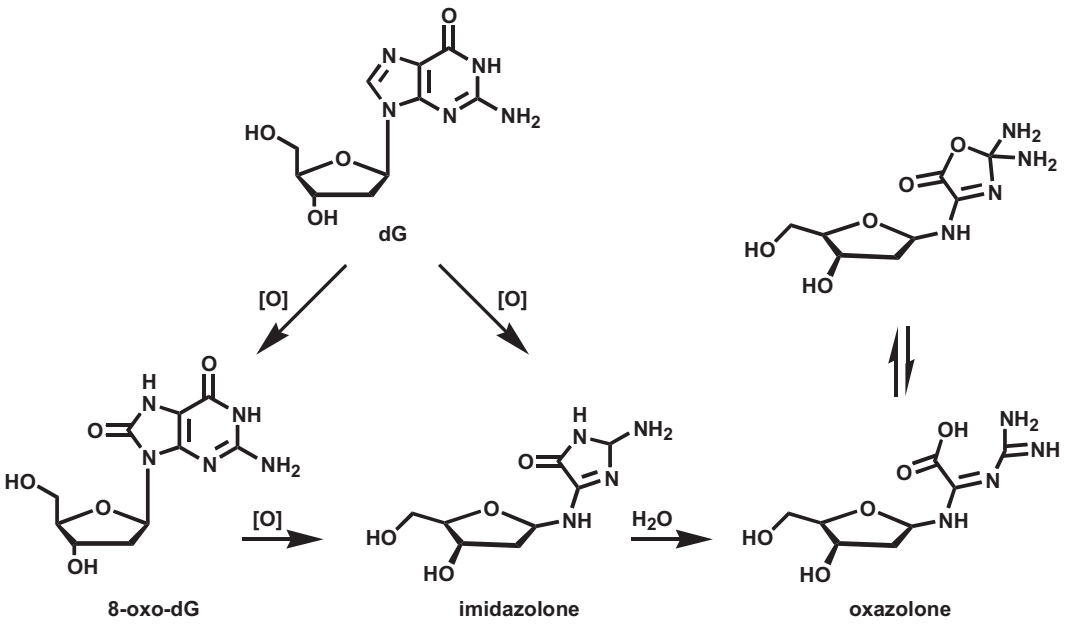

Scheme 1. Chemical structures of the oxidative DNA lesions examined in the present study.

carcinogenic risk indicators (1,20,21). 8-Oxo-dG is commonly used as a marker of DNA oxidation, mainly because of its prevalence and the ease of its measurement by high-performance liquid chromatography (HPLC) with electrochemical detection (22). For example, 8-oxo-dG levels have been reported to be increased in leukocyte DNA of smokers as compared with non-smoking controls (23). 8-Oxo-dG, however, is also produced as an artifact from normal 2′-deoxyguanosine during sample processing, leading to overestimation of its amounts (24). Large discrepancies in the levels of 8-oxo-dG determined by different laboratories are likely due to differences in analytical procedures including DNA extraction, hydrolysis and derivatization (20,22,24).

The use of 8-oxo-dG as a biomarker of DNA oxidation is further complicated by its facile oxidation in the presence of reactive oxygen and nitrogen species. Since 8-oxo-dG has a lower redox potential than normal guanine (0.58–0.75 V compared to 1.29 V for dG) (8,25,26), it is preferentially oxidized even in the presence of a large excess of normal guanines (27–29). 8-Oxo-dG has been proposed to act as a 'trap' for oxidative damage via the free radical or electron hole migration to 8-oxo-dG along the DNA duplex (8,15,17,29,30). In the event that 8-oxo-dG is specifically targeted for further oxidation *in vivo* upon long-term exposure of cellular DNA to oxidants, its use as a biomarker of oxidative stress may be misleading. On the other hand, the secondary products resulting from further oxidation of 8-oxo-dG, e.g. oxazolone, oxaluric acid, cyanuruc acid, guanidinohydantoin, 5-guanidino-4-nitroimidazole and urea, are mispairing lesions that may, in turn, play a role in mutagenesis of reactive oxygen species (ROS) (31–35).

Oxazolone is generated *via* spontaneous hydrolysis of imidazolone, which can be produced directly by oxidation of guanine nucleobases in DNA or as a secondary oxidation product with an intermediate of 8-oxo-dG (Scheme 1) (10,18,19,36). Imidazolone and oxazolone lesions have been found in DNA following exposure to Type I photo-oxidizing agents, ionizing radiation, superoxide radicals and peroxynitrite (14,37–40). Kino and Saito (10) proposed that imidazolone and oxazolone nucleosides may be responsible for the formation of piperidine-sensitive alkali-labile sites at the 5′-guanine of 5′-GG-3′ sequences following one-electron oxidation of DNA. These and other investigators have shown that synthetic DNA oligomers containing oxazolone are quantitatively cleaved by hot piperidine treatment at the oxidized nucleotide, while the strand scission of the corresponding 8-oxo-dG-containing oligonucleotides is inefficient (10,41). Therefore, oxazolone formation may be the underlying basis for the formation of single-strand breaks following hot piperidine treatment of ROS-treated DNA, a procedure commonly used to assess oxidative DNA damage (42).

Primer extension studies and site-specific mutagenesis experiments using synthetic oxazolone-containing DNA indicate that oxazolone is at least an order of magnitude more mutagenic than 8-oxo-dG, giving rise to G→T transversions (31,43). This suggests that, if formed *in vivo*, oxazolone may play a role in oxidative stress-related mutations and cancer. Yu *et al*. (38) reported recently the use of HPLC-MS/MS to quantify oxazolone lesions in calf thymus DNA treated with varying concentrations of peroxynitrite. However, to our knowledge, there are no previous reports of oxazolone formation in cellular DNA. It is possible that oxazolone has not been detected among DNA lesions *in vivo* because of its low yield as compared with 8-oxo-dG, its efficient repair (41,43), hydrolytic instability (36) or insufficiently sensitive analytical methods for its detection.

The goal of the present investigation was to establish whether oxazolone lesions are present in cellular DNA and to determine their potential usefulness as a biomarker of DNA oxidation. Previous studies demonstrated that 8-oxo-dG and other oxidative lesions are present in normal tissues of humans and laboratory animals with no known exposure,

probably as a result of background DNA oxidation by endogenous ROS (20,22,24). The present study uses liver DNA isolated from streptozotocin-induced diabetic rats exhibiting high levels of oxidative stress and lipid peroxidation (44,45). Our approach is based on sensitive and specific detection of 8-oxo-dG and oxazolone in enzymatic DNA digests by isotope dilution HPLC-ESI-MS/MS following a two-step off-line HPLC cleanup. Both 8-oxo-dG and oxazolone were detected in liver DNA of control and diabetic rats. The presence of oxazolone in DNA from an *in vivo* source suggests a possible role for this oxidative nucleobase lesion in mutagenesis induced by reactive oxygen and nitrogen species.

MATERIALS AND METHODS

Chemicals

Ammonium acetate, acetonitrile, methanol, magnesium dichloride and the Tris base (Fisher Scientific, Hanover Park, IL); calf thymus DNA, riboflavin, 8-oxo-dG, alkaline phosphatase, manganese(IV) oxide, TEMPO and 2′-deoxyguanosine (Sigma-Aldrich, Milwaukee, WI); guanidine thiocyanate (Promega Corporation, Madison, WI); DNase I and Phosphodiesterases I and II (Worthington Biochemicals, Lakewood, NJ); and $^{15}N_5$-dGTP (Martek, Columbia, MD) were from the sources indicated. Phase lock gel (heavy) tubes (15 ml) were from Eppendorf (Hamburg, Germany).

$^{15}N_5$-dG: $^{15}N_5$-dGTP (5 mg) was dissolved in 200 µl of 50 mM Tris–HCl/1 mM $MgCl_2$ buffer, pH 9, and incubated with alkaline phosphatase (75 U) for 5 h at 37°C. The hydrolysates were subjected to an HPLC using an Agilent Eclipse XDB-C8 column (4.6 × 150 mm, 5 µm) and a gradient of acetonitrile (solvent B) in 150 mM ammonium acetate (solvent A) at a flow rate of 1 ml/min. The solvent composition was as follows: 0–2 min, 0% B; 15 min, 3% B; 18 min, 30% B; 25 min, 30% B. The peak corresponding to $^{15}N_5$-dG (t_R=12 min) was collected and concentrated under reduced pressure. The identity and purity of $^{15}N_5$-dG was confirmed by UV spectrophotometry, molecular weight from ESI^+ MS and MS/MS fragmentation pattern.

Oxazolone and $^{15}N_4$ –oxazolone were prepared by riboflavin-mediated photooxidation of 2′-dG or $^{15}N_5$-dG, respectively. 2′-dG or $^{15}N_5$-dG was dissolved in 800 µl of a saturated aqueous solution of riboflavin and placed in a glass scintillation vial. The solution was continuously purged with air, while it was irradiated for 1 h with a 75 W tungsten lamp placed at 5 cm from the vial. The photooxidation mixtures were separated by HPLC using the column and solvent gradient described above. The peaks corresponding to imidazolone (t_R = 3.2 min) and oxazolone (t_R = 1.9 min) (Figure 1a) were collected and kept overnight at room temperature to convert imidazolone to oxazolone. Oxazolone was further purified by HPLC using a Thermo Hypersil-Keystone Hypercarb column (2.1 × 100 mm, 5 µm) and a linear gradient of acetonitrile in water (3–9% in 10 min) at a flow rate of 0.3 ml/min. The identities of purified oxazolone (t_R = 6.4 min) and $^{15}N_4$-oxazolone were established by UV spectrophotometry (Figure 1b), proton NMR and ESI^+ MS (Figure 2). The amount of unlabeled oxazolone in $^{15}N_4$-oxazolone stock solution was <0.65% as determined by ESI^+ MS analysis. Concentrations of oxazolone in stock solutions were determined by UV spectrophotometry using the extinction coefficient $\varepsilon_{233} = 1.833\ mM^{-1}\ cm^{-1}$.

$^{15}N_5$-8-oxo-dG was prepared by H_2O_2-mediated oxidation of $^{15}N_5$-dG in the presence of ascorbic acid (46). A mixture containing 1.3 mM $^{15}N_5$-dG, 10 mM ascorbic acid and 50 mM H_2O_2 in 0.1 M sodium phosphate, pH 6.8, was incubated for 4 h at 37°C. $^{15}N_5$-8-Oxo-dG was purified by HPLC using the column and gradient described for $^{15}N_5$-dG above. The peak of $^{15}N_5$-8-oxo-dG (t_R = 15.3 min) was collected and dried under reduced pressure. The identity of the standard was established by UV spectrophotometry and MS. ESI MS of $^{15}N_5$-8-oxo-dG: *m/z* 289.2 $[M + H]^+$, 173.2 $[M + 2H - dR]^+$. The amount of unlabeled 8-oxo-dG in $^{15}N_5$-8-oxo-dG stock solution was <0.1% by ESI^+ MS analysis. Concentrations of 8-oxo-dG in standard solutions were determined by UV spectrophotometry ($\varepsilon_{294} = 9700\ M^{-1}\ cm^{-1}$) (47).

Photooxidation of DNA

A glass vial containing 1 mg/ml of calf thymus DNA dissolved in a saturated aqueous solution of riboflavin was placed in ice-cold water. The solution was irradiated using a 75 W tungsten bulb positioned at ~5 cm from the vial. The reaction mixture was continuously purged with a steady stream of air. Aliquots of 50 µl were withdrawn at 0, 5, 10, 15, 20, 30 and 60 min. The DNA was precipitated with cold ethanol.

Animals and treatment

The use of female Sprague–Dawley rats (Harlan Sprague Dawley, Indianapolis, IN) was approved by the University of Minnesota Institutional Animal Care and Use Committee. Starting at 3 weeks of age, rats were fed a 10% beef tallow-based diet for a total of 13 weeks as described previously (44). Rats were injected intraperitoneally with two doses of streptozotocin (40 mg/kg body weight at 6 weeks of age and an additional dose of 50 mg/kg body weight at 8 weeks of age) to induce diabetes or saline (0.9% NaCl in water, pH 7.4). Feeding was continued for another 4 weeks. At the end of week 13, rats were fasted for 48 h and euthanized as described previously (44). The livers were collected, frozen and stored at −70°C.

DNA extraction from rat liver

A modification of the method described by Hofer and Möller (48) was used. To minimize oxidation of DNA during the extraction procedure, all solutions were saturated with argon (Ar) and kept on ice. TEMPO (5 mM) was added to all buffers as an antioxidant. Rat liver tissue (0.25–1 g) was placed in a glass/glass homogenizer with 10 ml of homogenization buffer (20 mM Tris–HCl, pH 7.5, containing 5 mM $MgCl_2$ and 5 mM TEMPO), and homogenized with ~10 strokes. The homogenates were transferred to a centrifuge tube and centrifuged at 1000 *g* for 10 min at 4°C. The nuclear pellets were suspended in 10 ml of the above homogenization buffer containing 0.5% v/v Tween-20 and centrifuged at 1000 *g* for 10 min at 4°C. This procedure was repeated two more times. After the final extraction, the nuclear pellet was dissolved in 5 ml of 4 M guanidine thiocyanate and transferred to a 15 ml phase lock gel (heavy)

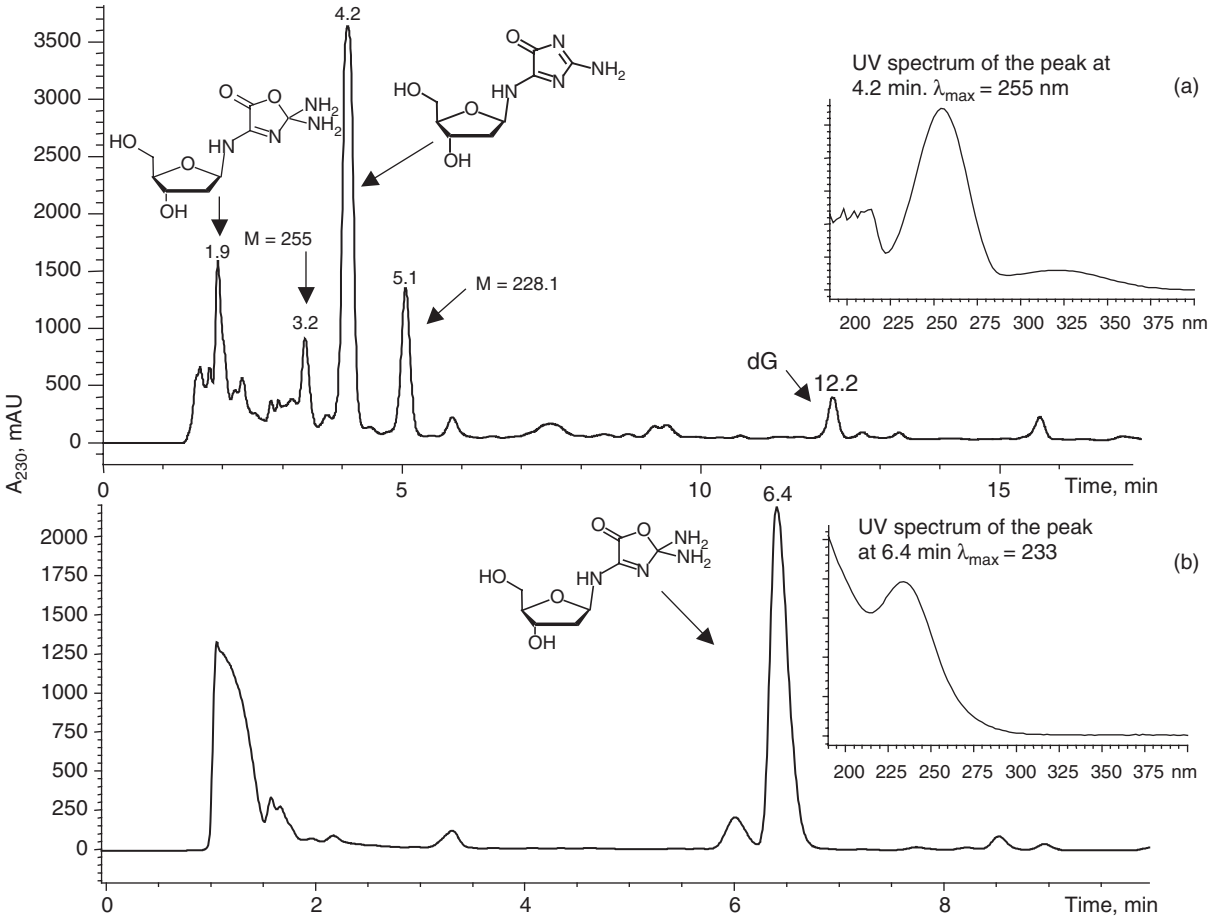

Figure 1. HPLC separation of the products resulting from dG photooxidation in the presence of riboflavin: (**a**) Separation of crude reaction mixtures by reversed phase HPLC. An Agilent Eclipse XDB-C8 column was eluted with a gradient of acetonitrile in 150 mM ammonium acetate. (**b**) Further purification of oxazolone on a carbon column. A Thermo Hypersil-Keystone Hypercarb column was eluted with a gradient of acetonitrile in water.

Eppendorf tube. Each sample was mixed with 5 ml of Sevag (a 1:24 mixture of isoamyl alcohol in chloroform) and the tube was shaken by hand for 1 min. After centrifugation at 1500 *g* for 5 min at 4°C, the aqueous phase was transferred to a clean centrifuge tube. The DNA was precipitated with 5 ml of isopropanol under Ar atmosphere overnight at −20°C. The DNA was pelleted by centrifugation for 15 min at 9000 *g* at 4°C. The residual isopropanol was evaporated under a flow of nitrogen, and the DNA pellet was resuspended in 1 ml of homogenization buffer and transferred to a clean microcentrifuge tube. RNase A (140 U) and RNase T_1 (1600 U) were added, followed by incubation at 37°C for 3 h. Proteinase K (40 U) was then added and the mixture was incubated for additional 2 h while gently shaken every 15 min. After incubation, the mixture was transferred to a 15 ml phase lock gel tube (heavy) and 4 ml of 4 M guanidine thiocyanate was added. Each sample was then mixed with 5 ml of Sevag and the tube were shaken by hand for 1 min. After centrifugation at 1500 *g* for 5 min at 4°C, the aqueous phase was transferred to a clean centrifuge tube. The DNA was precipitated with isopropanol under Ar atmosphere for 30 min at −20°C. The supernatant was removed and the pellet was washed with 70% aqueous ethanol. After centrifugation at 9000 *g* at 4°C for 15 min, the DNA pellet was dried under Ar and dissolved in water. DNA concentration was determined by UV absorption (A_{260} = 1 for 50 μg DNA). Typical A_{260}/A_{280} values were between 1.6 and 1.8.

Enzymatic hydrolysis of DNA

DNA samples (0.1 mg) from either *in vivo* or *in vitro* sources were dissolved in 150 μl of 10 mM Tris–HCl buffer (pH 7) containing 15 mM $MgCl_2$ and 5 mM TEMPO, and spiked with known amounts of isotopically labeled internal standards of $^{15}N_5$-8-oxo-dG and $^{15}N_4$-oxazolone (12 pmol each for *in vitro* samples, 1–2 pmol each for *in vivo* samples). DNA hydrolysis was performed by adding a mixture of DNase I (4 U), phosphodiesterase I (32 mU), phosphodiesterase II (80 mU) and alkaline phosphatase (16 U), followed by incubation for 8–10 h at 37°C (22). All reagents were scaled accordingly when using different DNA amounts.

To ensure the completeness of enzymatic hydrolysis, small aliquots of the digests were analyzed by HPLC-UV using the column (an Eclipse XDB-C8) and solvent gradient described for $^{15}N_5$-dG above. Under these conditions, normal DNA nucleosides eluted in the following order: dC, 6 min; dG, 12.3 min; dT, 14.4 min; and dA, 18.4 min. In some cases, 2′-deoxyinosine (dI) was also observed, eluting at 11.6 min.

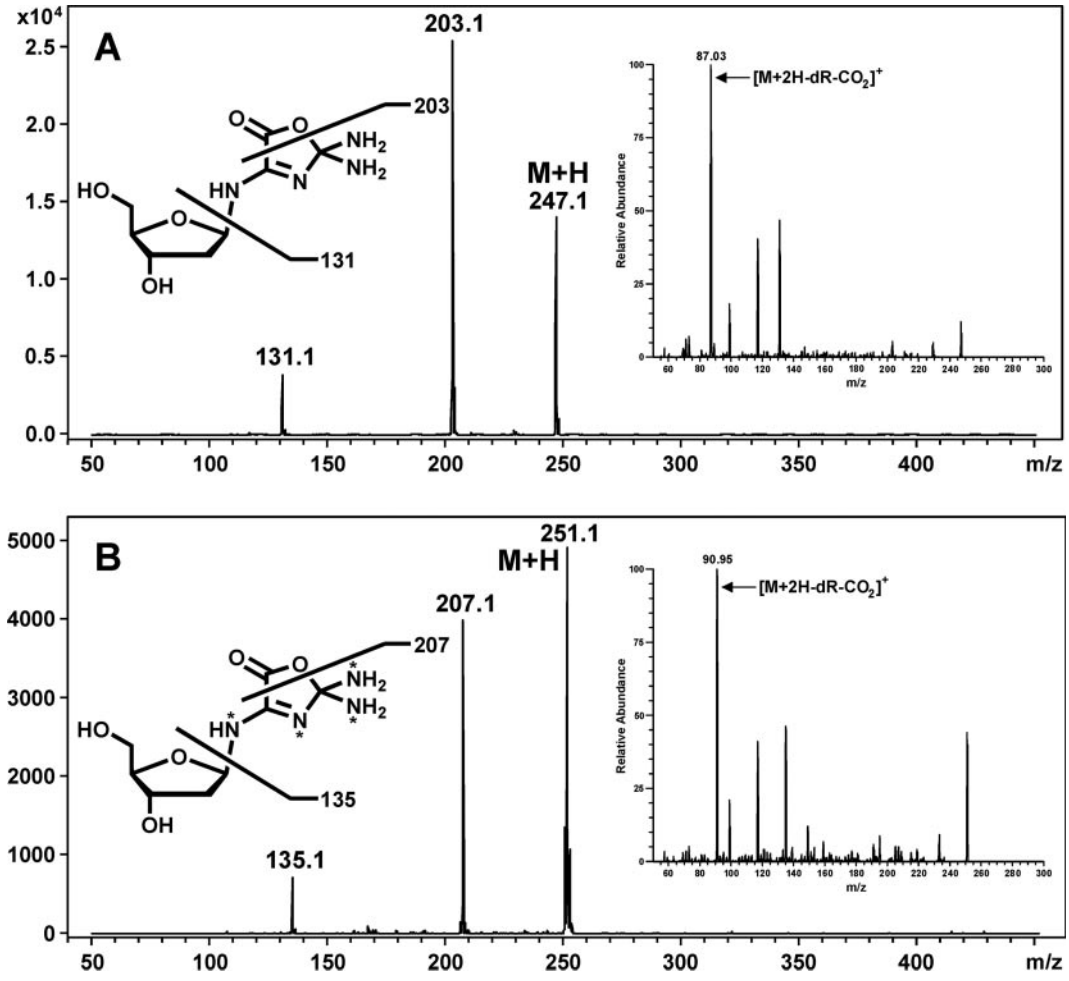

Figure 2. ESI$^+$ MS/MS spectra of oxazolone (**a**) and [$^{15}N_4$]-oxazolone (**b**) obtained at a low collision energy and at a higher collision energy (insert).

dI is produced by deamination of 2′-deoxyadenosine by deaminases present in commercial alkaline phosphatase preparations (49,50). No attempt was made to inhibit this artifactual deamination as it did not interfere with quantification of oxazolone and 8-oxo-dG (data not shown). If RNA contamination was observed, RNA nucleosides eluted as follows: cytidine, 3.7 min; uridine, 5.5 min; guanosine, 10.5 min; adenosine, 18 min. Samples exhibiting RNA contamination were not further analyzed. Test experiments employing imidazolone standard have shown that imidazolone was quantitatively converted to oxazolone under the conditions of enzymatic hydrolysis. Upon completion of hydrolysis, samples were divided into two equal parts for 8-oxo-dG and oxazolone analyses. DNA hydrolysates from *in vitro* experiments were analyzed directly after filtration through Microcon YM-30 centrifugal filters (Millipore Corporation, Bedford, MA) to remove proteins. The filters were pre-rinsed with water (6 × 500 µl) to remove glycerol. Analyses of 8-oxo-dG in rat liver DNA were performed directly without further purification. Quantification of oxazolone in the rat liver DNA was carried out following offline HPLC purification as described below.

Offline HPLC purification of oxazolone from enzymatic digests of rat liver DNA

Sample volume was adjusted to 500 µl with Milli-Q water, and the samples were loaded onto an Agilent XDB-C8 column (4.6 × 100 mm, 5 µm) eluted with the solvent system of 15 mM ammonium acetate (A) and acetonitrile (B) at a flow rate of 1 ml/min. The solvent composition was held at 0% B for 2.5 min, and then changed linearly to 4.5% B at 21.5 min and further to 30% B at 24.5 min. Fractions containing oxazolone and [$^{15}N_4$]-oxazolone (1.55–3 min) were collected, dried under vacuum and redissolved in 500 µl of acetontrile/methanol (3:1) for the second purification by normal phase HPLC. Samples were loaded onto a Waters (Milford, MA) Atlantis Hilic silica column (2.1 × 150 mm, 5 µm) and eluted with a gradient of acetonitrile (solvent A) in nanopure water (solvent B) (0 min, 10% B; 18 min, 28% B; 19 min, 10% B) at a flow rate of 0.3 ml/min. Under these conditions, oxazolone standard eluted at 15.1 min. To insure complete collection of oxazolone and its ^{15}N-internal standard, HPLC fractions were collected from 14 to 16.9 min. HPLC fractions were dried under vacuum and redissolved in 20 µl of nanopure water for HPLC-ESI-MS/MS analysis.

Blank injections were performed periodically to check for any cross-contamination.

Capillary HPLC-ESI-MS/MS

Oxazolone analysis was performed with a Thermo-Finnigan TSQ Quantum Ultra mass spectrometer interfaced with an Agilent 1100 capillary HPLC. A Thermo Hypersil-Keystone (Bellefonte, PA) Hypercarb column (0.5 × 100 mm, 5 μm) was eluted with a gradient of isopropanol/acetonitrile (3:1) (solvent B) in 0.05% acetic acid (solvent A) (0 min, 0% B; 1 min, 0% B; 8.5 min, 10.7% B; 9.3 min, 0% B; 20 min, 0% B) at a flow rate of 12 μl/min. The mass spectrometer was operated in the ESI^+ MS/MS mode. The spray voltage was set to 3.1 kV, the source temperature was 250°C, and the sheath gas pressure was 30 psi. Product ions of *m/z* 247.1 ($[M + H]^+$ of oxazolone nucleoside) and *m/z* 251.1 ($^{15}N_4$-oxazolone, internal standard) were obtained, with a collision energy of 14 and a collision gas pressure of 1 mtorr. The peak width for Q1 and Q3 were both set to 0.70 amu. Quantitative analyses were performed in selected reaction monitoring mode using the transitions *m/z* 247.1→87.1 $[M + 2H - dR - CO_2]^+$ and *m/z* 251.1→91.1 for oxazolone and $^{15}N_4$-oxazolone, respectively. The method was validated by spiking calf thymus DNA (0.2 mg) with 2 pmol each oxazolone and $^{15}N_4$-oxazolone, followed by enzymatic hydrolysis, HPLC cleanup and HPLC-ESI^+-MS/MS analysis as described above (Scheme 2). Spiked samples were quantified to contain 96.7 ± 1.3% of the target oxazolone amount ($n = 5$). The same experiment performed in the absence of DNA (pure standards) yielded an accuracy of 100–103%, with a precision of 2.62% ($N = 8$, during several days). The lower limit of detection for oxazolone standard was estimated as 5 fmol on column ($S/N = 4$).

Quantification of 8-oxo-dG was achieved with an Agilent 1100 capillary HPLC-ion trap MS. An Agilent Zorbax SB C18 column (0.5 × 150 mm, 5 μm) was maintained at 10°C. The column was eluted with a gradient of methanol (solvent B) in 15 mM ammonium acetate (solvent A) (0 min, 3% B; 18 min, 11% B; 30 min, 70% B) at a flow rate of 12 μl/min. The mass spectrometer was operated in the ESI^+ MS/MS mode. The skimmer and capillary exit voltages were maintained at 26.8 and 96.9 V, respectively. The accumulation time was 300 ms. Product ions of *m/z* 284.1 (8-oxo-dG) and 289.1 ($^{15}N_5$-8-oxo-dG, internal standard) were obtained with a fragmentation amplitude of 0.79. Quantitative analyses were performed in selected reaction monitoring mode using the transitions *m/z* 284.1→168.0 $[M + 2H - dR]^+$ for 8-oxo-dG and the corresponding transition *m/z* 289.1→173 for $^{15}N_5$-8-oxo-dG (internal standard). The method was validated by spiking calf thymus DNA (1 mg) with 8-oxo-dG standard (10 pmol), followed by enzymatic hydrolysis and HPLC-ESI-MS/MS analysis as described above. Control material was quantified to contain 98–111% of the target amount with a precision of 7.03% ($n = 5$).

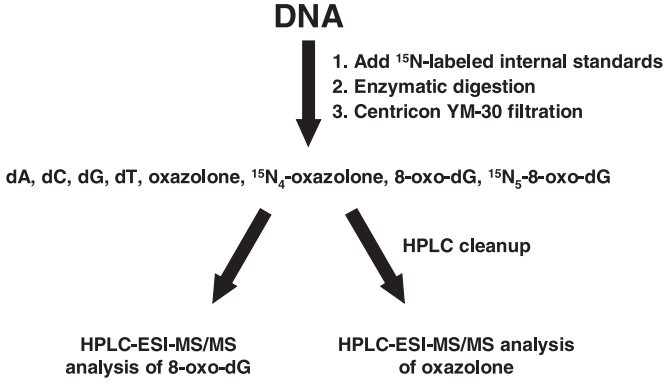

Scheme 2. Experimental scheme for HPLC-ESI-MS/MS analysis of 8-oxo-dG and oxazolone in DNA.

RESULTS

Synthesis and structural characterization of oxazolone and $^{15}N_4$-oxazolone

Authentic standards of oxazolone and $^{15}N_4$-labeled oxazolone were synthesized by photooxidation of dG or $^{15}N_5$-dG in the presence of riboflavin. Crude reaction mixtures were separated on a reversed phase C8 HPLC column (Agilent Eclipse XDB-C8) and the identity of each HPLC peak was established from the UV and ESI^+ MS spectra (Figures 1 and 2). Imidazolone (M = 228, MS/MS *m/z* 229 $[M + H]^+$→113 $[M + 2H - dR]^+$) was the major product (50–70% yield) eluting at 4.2 min at our conditions (Figure 1). Minor products found in the photooxidation mixtures were (2S)-2,5′-anhydro-1-(2′-deoxy-β-D-*erythro*-pentofuranosyl)-5-guanidinylidene-2-hydroxy-4-oxoimidazolidine (M = 255, MS/MS *m/z* 256 $[M + H]^+$→140 $[M + 2H - dR]^+$ (51) eluting at 3.2 min and the α-furanose anomer of imidazolone (40) eluting at 5.1 min (Figure 1a).

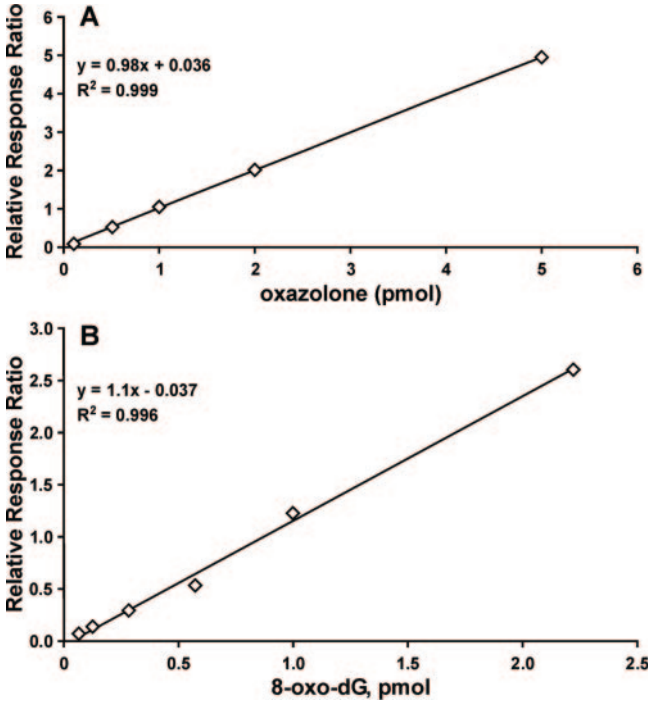

Figure 3. Calibration curves for isotope dilution capillary HPLC-ESI^+ MS/MS analysis of oxazolone (**a**) and 8-oxo-dG (**b**). Internal standard amounts were 1 pmol for [$^{15}N_5$]-8-oxo-dG and 2 pmol for [$^{15}N_4$]-oxazolone.

Isolation of oxazolone nucleoside by HPLC was complicated by its early elution from the reversed phase HPLC column (t_R = 1.9 min, Figure 1a). The majority of previous studies have employed acetylated nucleosides to facilitate HPLC separation of the polar dG oxidation products (19). Since acetyl groups would interfere with our ability to use the synthetic compound as a standard for quantification of oxazolone in DNA hydrolysates, an alternative approach using non-acetylated nucleosides was required. Our purification procedure of free oxazolone nucleoside included two HPLC steps. HPLC fractions corresponding to imidazolone nucleoside (t_R = 4.2 min, Figure 1a) were collected and kept at room temperature overnight to achieve hydrolytic conversion of imidazolone to oxazolone (Scheme 1). Further purification of oxazolone was accomplished with the use of a highly hydrophobic Hypercarb column (Thermo Hypersil-Keystone) (32), which allowed retention of the oxidized nucleoside (t_R = 6.4 min, Figure 1b). The purity of oxazolone standard was confirmed by UV spectrophotometry (Figure 1b, inset), mass spectrometry (Figure 2) and proton NMR (500 MHz ^{1}H NMR data in ^{6}DMSO: (δ) 8.05 d 1H J = 9.3, 4-NH; (δ) s 4H, NH_2; (δ) 5.6 m 1H, $J_{1'-2'}$ = 7.5, $J_{1'-2'}$ = 6.2, H-1′; (δ) 5.0 d 1H, J = 4.05, CHO**H**-3′; (δ) 4.7 d 1H, J = 5.6, CHO**H**-5′; (δ) 4.1 m 1H, H-3′; (δ) 3.6 m 1H, $J_{3'-4'}$ = 2.5, $J_{4'-5''}$ = 5.0, H-4′; (δ) 3.4 m 1H, H-5′; (δ) 3.3 m 1H, H-5″; (δ) 2.1 dd 1H, H-2′; (δ) 2.0 dd 1H, H-2″) and mass spectrometry (Figure 2a). Concentrations of oxazolone in stock solutions were determined by UV spectrophotometry (ε_{233} = 1.833 mM^{-1} cm^{-1}). ^{15}N-labeled oxazolone for use as HPLC-ESI-MS/MS internal standard was prepared by the same procedure starting with $^{15}N_5$-dG (Figure 2b).

Quantitative HPLC-ESI$^+$-MS/MS method development for assays of oxazolone and 8-oxo-dG

We employed HPLC-ESI$^+$-MS/MS because this methodology does not require chemical derivatization of oxidized nucleosides and affords adequate sensitivity for analyses of DNA adducts from *in vivo* sources. Our typical detection limits for covalently modified DNA nucleosides are 5–20 fmol per 100 μg of DNA.

Our experimental procedures for quantitative analysis of 8-oxo-dG and oxazolone in DNA hydrolysates are outlined in Scheme 2. Early in the analysis, DNA samples were spiked with a mixture of $^{15}N_4$ -oxazolone and $^5N_5$-8-oxo-dG which served as internal standards for capillary HPLC-MS/MS. DNA was enzymatically digested in the presence of PDE I, PDE II and DNase at pH 7.0. Our control experiments (data not shown) confirmed that under these conditions, imidazolone was completely converted to oxazolone, but no further degradation of oxazolone nucleoside occurred. No attempt was made to develop quantitative assay for imidazolone because of its inherent instability at physiological conditions. Aliquots of enzymatic digests were analyzed by HPLC-UV to ensure the completeness DNA hydrolysis and to rule out any RNA contamination. Following ultrafiltration through Centricon YM-30 microfilters, samples were injected onto a capillary HPLC column for HPLC-ESI-MS/MS analysis (Scheme 2). 8-Oxo-dG was directly analyzed in crude DNA digests without any pre-purification or derivatization steps to minimize artifactual formation of 8-oxo-dG. To minimize DNA oxidation during enzymatic digestion, TEMPO (5 mM) was added to all buffers and all solutions were purged with argon. Samples were kept on ice and either analyzed on the same day or stored under Ar at −70°C for less than a week.

The MS/MS fragmentation pattern of oxazolone nucleoside (m/z ($[M+H]^+$) = 247.1) at low collision energies is characterized by two predominant fragmentation pathways (Figure 2a). The loss of a molecule of carbon dioxide leads to the major fragments at m/z 203.1. Unlike typical MS/MS spectra of native DNA nucleosides (52), product ions corresponding to the loss of deoxyribose (BH_2^+, m/z 131) are less abundant than the $[M+H\text{-}CO_2]^+$ fragments (Figure 2a). This distinct fragmentation pattern reflects the loss of aromaticity upon oxidation of dG to oxazolone, accompanied by the incorporation of relatively labile lactone group in the molecule (Scheme 1). At high collision energies, one major fragment at m/z 87.1 predominated $[M + 2H - dR - CO_2]^+$.

Mass spectral analysis of ^{15}N-labeled oxazolone standard (Figure 2b) confirmed the presence of four ^{15}N atoms in the molecule (M = 250.1 versus 246.1 for unlabeled oxazolone). Although the starting material ($^{15}N_5$-dG) contains five ^{15}N atoms, one of the nitrogens (the former N-7) was lost as $HCONH_2$ during oxazolone formation from dG (19). The observed (+4) mass shift for the mass fragments originating from $^{15}N_4$-oxazolone (Figure 2b) is consistent with the presence of four ^{15}N atoms in the molecule and the retention of these atoms in $[M + H - dR]^+$ (m/z 235) and $[M + H - CO_2]^+$ (m/z 207) ions. As was the case with unlabeled nucleoside, the major fragmentation process observed at high collision energies was the loss of deoxyribose and a molecule of carbon dioxide $[M + 2H - dR - CO_2]^+$ (m/z 91.1).

Our HPLC-ESI-MS/MS method for analysis of oxazolone is based on selected reaction monitoring of the transition m/z 247.1 $[M + H]^+ \rightarrow 87.1$ $[M + 2H - dR - CO_2]^+$ for $^{15}N_0$-oxazolone and the corresponding transition m/z 251.1→91.1 for the $^{15}N_4$-labeled internal standard. A capillary Hypercarb HPLC column (0.5 mm i.d.) is eluted at a flow rate of 12 μl/min with a gradient of isopropanol/acetonitrile (3:1) in 0.05% acetic acid. Our HPLC-ESI-MS/MS detection limit for oxazolone using the TSQ system was estimated as 10 fmol (S/N = 3).

Quantitative analyses of oxazolone in DNA from the *in vivo* sources required an additional offline HPLC purification step because of an interfering impurity present in rat liver DNA. Our offline HPLC purification scheme included the use of two different HPLC columns. DNA hydrolysates were first loaded onto a reversed phase C8 HPLC column to remove the bulk of normal nucleosides. HPLC fractions corresponding to the expected elution time for oxazolone were collected, dried under vacuum and further separated with a Waters (Milford, MA) Atlantis Hilic silica column (2.1 × 150 mm, 5 μm) eluted with a gradient of acetonitrile in water. HPLC-purified samples were dried and reconstituted in 20 μl of water and injected onto capillary columns for HPLC-ESI-MS/MS analysis with a triple quadrupole mass spectrometer. Method was validated by spiking calf thymus DNA with known amounts of oxazolone and $^{15}N_4$-oxazolone. Method accuracy and precision were determined 96.7 ± 1.3%

($n = 5$). Similar analyses of pure standards provided an accuracy of 100.6–103% and a precision of 0.97%. Our optimized HPLC-ESI-MS/MS method was employed for analyses of oxazolone in rat liver DNA.

Development of quantitative HPLC-ESI$^+$-MS/MS method for assays of 8-oxo-dG

In addition to oxazolone, 8-oxo-dG was quantified in each DNA sample. Our HPLC-ESI-MS/MS method for 8-oxo-dG employed selected reaction monitoring of the transitions 284.2 $[M + H]^+ \rightarrow 168.2$ $[M + 2H - dR]^+$ (8-oxo-dG) and 289.2 $[M + H]^+ \rightarrow 173.2$ $[M + 2H - dR]^+$ ($^{15}N_5$ –8-oxo-dG) on an Agilent 1100 capillary HPLC- Ion Trap MS system. HPLC separation was performed with a capillary Zorbax SB-C18 column. The use of a reduced temperature (10°C) was required to achieve complete separation of 8-oxo-dG from normal DNA nucleosides. Previous investigators have noted the ability of dG to oxidize to 8-oxo-dG in the ion source of the mass spectrometer, potentially interfering with quantitative analyses (22,53). Our attempts to remove dG by solid phase extraction on C18 cartridges proved unsuccessful. Therefore, efficient HPLC separation of 8-oxo-dG from dG during HPLC-ESI-MS/MS analyses was necessary. A series of pilot experiments using enzymatic digests of calf thymus DNA spiked with authentic 8-oxo-dG were performed to ensure efficient HPLC separation and accurate quantification of 8-oxo-dG in the presence of a large excess of dG and other native DNA nucleosides. The use of a Zorbax SB-C18 column with a gradient of acetonitrile in ammonium acetate at 10°C has afforded the necessary separation without the loss of HPLC resolution (Supplementary Data). 8-Oxo-dG detection limit on the ion trap system was calculated as 30 fmol ($S/N = 3$).

Tests for artifactual oxazolone formation from dG and 8-oxo-dG

In order to evaluate potential artifactual formation of oxazolone from dG during sample processing, rat liver DNA (250 μg, in duplicate) was spiked with synthetic DNA oligodeoxynucleotide containing [$^{14}N_4$]-dG (5 nmol), and the samples were processed and analyzed as described above. $^{15}N_3$-oxazolone formation was analyzed by monitoring the MS/MS transition m/z 250.1 $[M + H]^+ \rightarrow 90.1$ $[M + 2H - dR - CO_2]^+$. Under our conditions, no artifactual oxazolone was detected.

To test for possible formation of oxazolone from 8-oxo-dG during sample processing, 8-oxo-dG standard (100 nmol) was dissolved in 250 μl of the digestion buffer containing nuclease enzymes and incubated at 37°C for 18 h to imitate enzymatic digestion conditions. Following incubation, the sample was spiked with $^{15}N_3$ oxazolone (5 pmol) and subjected to the same HPLC cleanup as that for DNA from the *in vivo* sources (see above). Oxazolone formation was analyzed by monitoring the MS/MS transition m/z 247.1 $[M + H]^+ \rightarrow 88.1$ $[M + 2H - dR - CO_2]^+$. The amount of oxazolone produced from 100 nmol of 8-oxo-dG was 19.7 pmol (~0.02% conversion). Based on the amounts of 8-oxo-dG present in rat liver samples (1.1 pmol in 0.1 mg DNA), artifactual formation of oxazolone from 8-oxo-dG is negligible under the conditions of our experiments.

HPLC-ESI$^+$-MS/MS quantification of 8-oxo-dG and oxazolone in photooxidized DNA

The newly developed HPLC-ESI-MS/MS methods were tested by analyzing 8-oxo-dG and oxazolone in calf thymus DNA subjected to photooxidation in the presence of riboflavin. Riboflavin is an endogenous cellular photosensitizer that acts *via* the Type I mechanism, directly transferring a single electron from guanine molecule to the excited molecule of the dye (37). This initiates a series of reactions, ultimately leading to 8-oxo-dG and oxazolone (36,39). Under our experimental conditions (0°C, constant purging with air), amounts of oxazolone in DNA increased linearly with the duration of exposure to visible light (5–60 min irradiation, Figure 4). At short incubation times (0–20 min), 8-oxo-dG levels were comparable to those of oxazolone. When photooxidation time was extended to 30–60 min, oxazolone amounts continued to increase, suggesting that it was refractory to further oxidation in the presence of Type I photooxidizing agents (Figure 4). In contrast, 8-oxo-dG amounts reached a plateau following 20 min reaction, probably as a result of its oxidation to secondary products. Taken together with validation experiments described above, these *in vitro* studies confirmed that our HPLC-ESI-MS/MS methodology could be used for accurate and reliable quantification of both oxidative lesions in DNA hydrolysates from rat tissues.

HPLC-ESI$^+$-MS/MS analysis of oxazolone and 8-oxo-dG in rat liver DNA

The formation of 8-oxo-dG and oxazolone in DNA isolated from livers of control and diabetic rats maintained on a high fat, beef tallow-based diet was examined. A previous study (45) revealed that diabetic rats excreted increased amounts of lipophilic aldehydes and related carbonyl compounds in their urine as an indication of elevated lipid peroxidation. Representative HPLC-ESI-MS/MS traces for analyses of 8-oxo-dG and oxazolone in rat liver samples are shown in Figures 5 and 6, respectively. Oxazolone amounts in rat liver

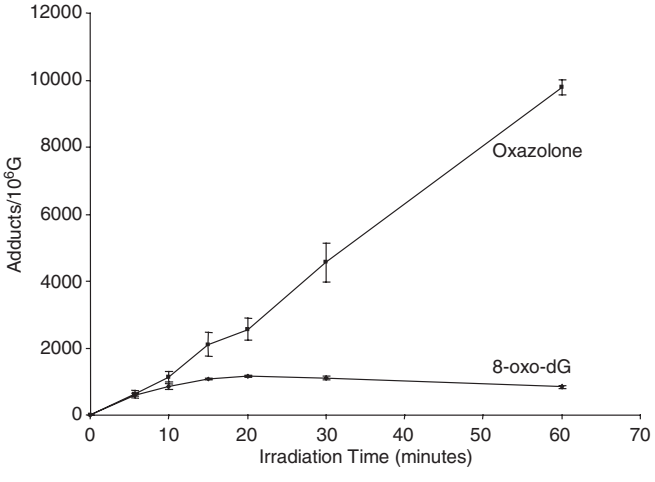

Figure 4. Formation of 8-oxo-dG and oxazolone in calf thymus DNA subjected to photooxidation in the presence of riboflavin. Aliquots of 50 μl were withdrawn at 0, 5, 10, 15, 20, 30 and 60 min, and analyzed as shown in Scheme 2.

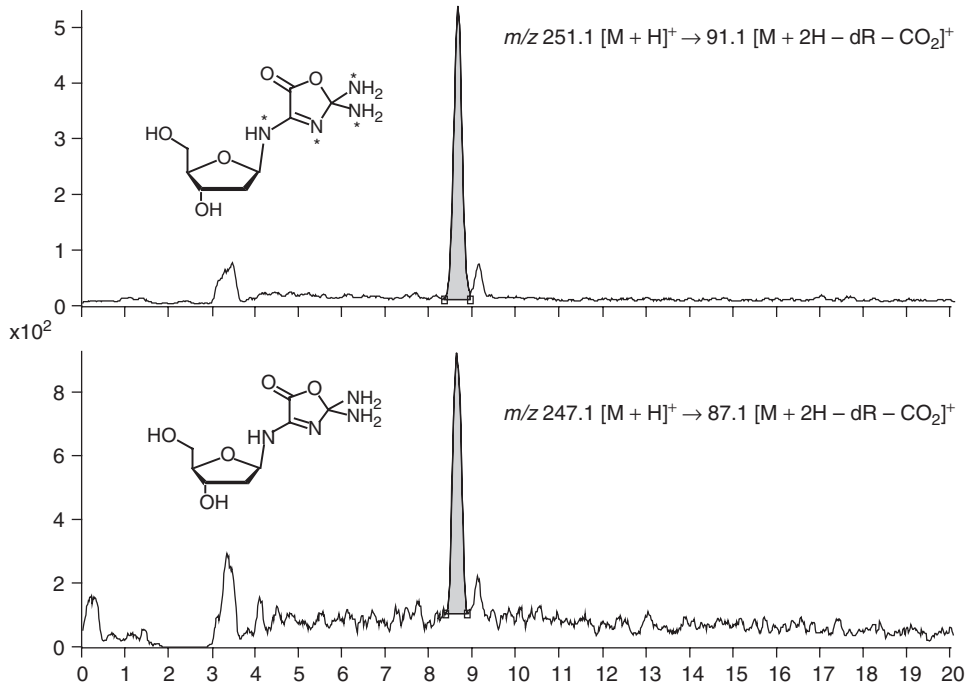

Figure 5. HPLC-ESI$^+$-MS/MS analysis of oxazolone in enzymatic hydrolysates of rat liver DNA (300 μg) following off-line HPLC purification (Scheme 2). An Agilent 1100 series capillary HPLC was interfaced to a Thermo-Finnigan TSQ Quantum Ultra mass spectrometer. A Thermo Hypersil-Keystone Hypercarb column (0.5 × 100 mm, 5 μm) was eluted at a flow rate of 12 μl/min with a gradient of isopropanol/acetonitrile (3:1) (solvent B) in 0.05% acetic acid (solvent A). The spray voltage was set to 3.1 kV, the source temperature was 250°C, and the sheath gas pressure was 30 psi. Quantitative analyses were performed in selected reaction monitoring mode using the transitions *m/z* 247.1→87.1 [M + 2H − dR − CO_2]$^+$, and *m/z* 251.1→91.1 for oxazolone and $^{15}N_4$-oxazolone, respectively.

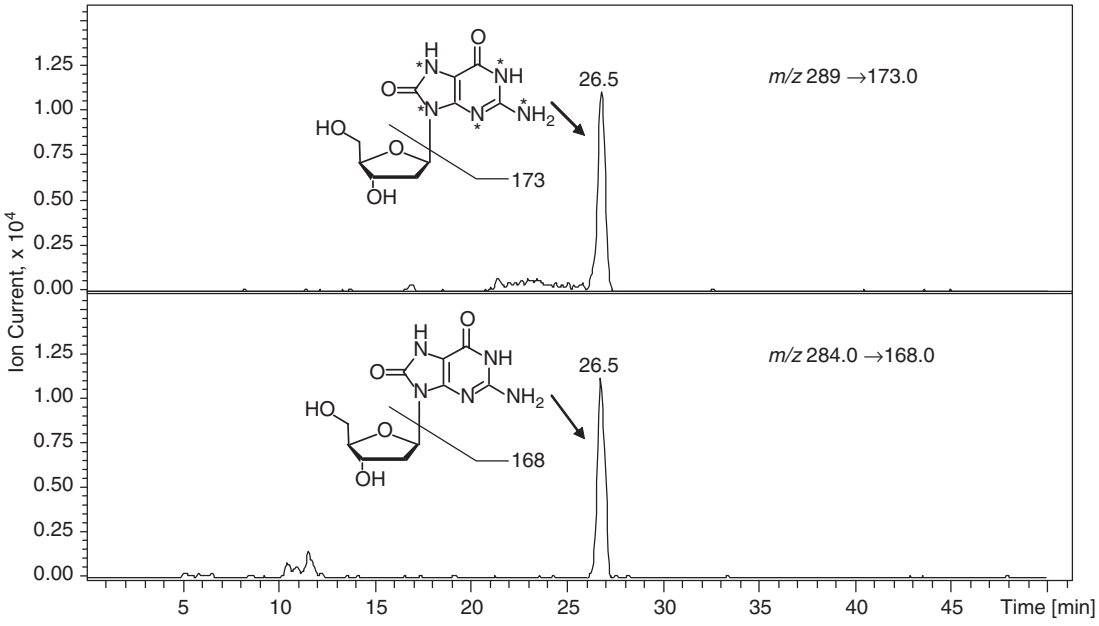

Figure 6. HPLC-ESI$^+$-MS/MS analysis of 8-oxo-dG in an enzymatic hydrolysate of rat liver DNA (80 μg). An Agilent 1100 series capillary HPLC-ion trap MS system was used. A Zorbax SB C18 column (0.5 × 150 mm, 5 (m) was maintained at 10°C and eluted at a flow rate of 12 (l/min with a gradient of methanol (solvent B) in 15 mM ammonium acetate (solvent A). The mass spectrometer was operated in the positive ion MS/MS mode. Quantitative analyses were performed in selected reaction monitoring mode using the transitions *m/z* 284.1→168.0 (M + 2H − dR)$^+$ for 8-oxo-dG and the corresponding transition *m/z* 289.1→173 for [$^{15}N_5$]-8-oxo-dG.

DNA (2–6 adducts per 10^7 normal guanines) were approximately an order of magnitude lower than those of 8-oxo-dG in the same tissue (3–8 adducts per 10^6 G) (Table 1). The levels of 8-oxo-dG detected in our study were similar to those determined by a similar method in the livers of control Sprague–Dawley rats (54). Streptozotocin-induced diabetic rats contained slightly higher levels of 8-oxo-dG than control animals ($P = 0.009$, Table 1), which was consistent with

Table 1. Quantitative analysis of 8-oxo-dG and oxazolone in DNA isolated from livers of control and diabetic rats maintained on beef tallow diet

Rats	8-Oxo-dG	Oxazolone
Control	4.63 ± 1.18 ($n = 4$)	0.41 ± 0.18 ($n = 4$)
Diabetic	7.46 ± 0.68[a] ($n = 3$)	0.51 ± 0.19[b] ($n = 3$)

Values (the mean ± SD) are the numbers of adducts per 10^6 normal guanines.
[a]$P = 0.009$ by two tail, unpaired *t*-test.
[b]$P = 0.5$ by two tail, unpaired *t*-test.

earlier reports of diabetes-induced increase in urinary 8-hydroxy-2′-deoxyguanosine (55). However, no significant differences were observed between oxazolone levels in liver DNA extracted from the two groups of animals ($P = 0.5$, Table 1).

DISCUSSION

Oxidative degradation of DNA appears to be causally involved in cancer and other human diseases (1–4,6,7,21). Guanine nucleobases are frequently targeted by oxidants due to their lowest redox potential among the DNA bases (6,9). Among guanine oxidation products, 8-oxo-7,8-dihydro-2′-deoxyguanosine (8-oxo-dG) is used widely as a biomarker of guanine oxidation because of its *in vivo* incidence and its facile measurement by HPLC with electrochemical detection (48). In contrast, another abundant oxidation product of guanine in DNA, oxazolone (Scheme 1), has received relatively little attention. Oxazolone was first discovered by Cadet *et al*. (19) as the major product of dG oxidation in the presence of hydroxyl radicals and photosensitizers. Kino and Saito (10) have demonstrated that the imidazolone precursor of oxazolone is also formed upon photooxidation of G-containing single-stranded synthetic oligodeoxynucleotides and proposed that the formation of these lesions, rather than 8-oxo-dG, is responsible for piperidine-sensitive alkali-labile sites in DNA subjected to photooxidation (10). Potent mispairing abilities of oxazolone have been demonstrated in site-specific mutagenesis experiments, where it led to ~10-fold more G to T transversions than 8-oxo-dG (31). Taken together, these results suggest that, if formed *in vivo*, oxazolone may play a role in mutagenesis by ROS.

The goal of the present study was to examine the occurrence of oxazolone in cellular DNA using highly sensitive and specific mass spectrometry-based methods. The analytical methodology developed in the present work allows a direct and accurate analysis of oxazolone in DNA samples from biological sources using stable isotope labeling - capillary HPLC-ESI$^+$-MS/MS. Our HPLC-ESI-MS/MS limit of detection for oxazolone was estimated as 5 fmol, with an accuracy of 96.7 ($n = 5$) and a precision of 1.3% ($n = 5$). While this manuscript was in preparation, Yu *et al*. (38) reported the development of a similar HPLC-ESI-MS/MS assay for oxazolone and its application to quantitative analysis of this lesion in DNA subjected to peroxynitrite treatment. However, to our knowledge, no previous reports of the *in vivo* formation of oxazolone are available in the literature.

Our results for dose-dependent formation of oxazolone and 8-oxo-dG in photooxidized calf thymus DNA are consistent with the earlier report of Kino and Sagiyama (56). These researchers employed HPLC with UV detection to monitor the formation of imidazolone and 8-oxo-dG in synthetic DNA duplexes irradiated in the presence of riboflavin. As in our study (Figure 4), the highest yields of 8-oxo-dG were observed at relatively short irradiation times, followed by a slow decline at prolonged irradiation (56). In contrast, Douki and Cadet (37) observed a linear increase in the amounts of both oxazolone and 8-oxo-dG in photooxidized DNA with increased irradiation time. This apparent discrepancy can be explained by differences in irradiation times used in these studies. Indeed, Douki and Cadet (37) stopped photooxidation at 20 min, i.e. before any non-linear behavior has been observed in our experiment (Figure 4).

To our knowledge, this report provides the first account of the formation of oxazolone *in vivo* (Figure 6 and Table 1). Although its levels were ~10-fold lower than those reported for 8-oxo-dG in this and other studies (54), oxazolone may be relevant for mutagenesis by ROS because of its mispairing potency (31) and its resistance to further oxidation (Figure 4). The reason for the lack of a significant difference between oxazolone amounts detected in liver DNA of diabetic and control rats examined in this study (Table 1) is as yet unclear. Future experiments with other animal models of oxidative stress will employ quantitative HPLC-ESI-MS/MS methods developed in the present work to help establish whether oxazolone can serve as a biomarker of DNA oxidation *in vivo*.

SUPPLEMENTARY DATA

Supplementary Data are available at NAR Online.

ACKNOWLEDGEMENTS

The authors thank Mr. Jeff Dahl (Univ. of Minnesota) for his assistance with photooxidation experiments, and Professor Steven Tannenbaum (MIT) for helpful discussions. Funding for this research was provided by a grant from the National Cancer Institute (CA095039), and Biomedical Research Funds, the US Department of Veterans Affairs.

Conflict of interest statement. None declared.

REFERENCES

1. Halliwell,B., Gutteridge,J.M. and Cross,C.E. (1992) Free radicals, antioxidants, and human disease: where are we now? *J. Lab. Clin. Med.*, **119**, 598–620.
2. Marnett,L.J. (2000) Oxyradicals and DNA damage. *Carcinogenesis*, **21**, 361–370.
3. Bennett,M.R. (2001) Reactive oxygen species and death—oxidative DNA damage in atherosclerosis. *Circulation Res.*, **88**, 648–650.
4. Canella,K.A., Diwan,B.A., Gorelick,P.L., Donovan,P.J., Sipowicz,M.A., Kasprzak,K.S., Weghorst,C.M., Snyderwine,E.G., Davis,C.D., Keefer,L.K. *et al*. (1996) Liver tumorigenesis by *Helicobacter hepaticus*: considerations of mechanism. *In Vivo*, **10**, 285–292.
5. Malins,D.C., Holmes,E.H., Polissar,N.L. and Gunselman,S.J. (1993) The etiology of breast cancer. Characteristic alteration in hydroxyl radical-induced DNA base lesions during oncogenesis with potential for evaluating incidence risk. *Cancer*, **71**, 3036–3043.
6. Greenberg,M.M. (2004) *In vitro* and *in vivo* effects of oxidative damage to deoxyguanosine. *Biochem. Soc. Trans.*, **32**, 46–50.
7. Paz-Elizur,T., Krupsky,M., Blumenstein,S., Elinger,D., Schechtman,E. and Livneh,Z. (2003) DNA repair activity for oxidative damage and risk of lung cancer. *J. Natl Cancer Inst.*, **95**, 1312–1319.

8. Prat,F., Houk,K.N. and Foote,C.S. (1998) Effect of guanine stacking on the oxidation of 8-oxoguanine in B-DNA. *J. Am. Chem. Soc*., **120**, 845–846.
9. Neeley,W.L. and Essigmann,J.M. (2006) Mechanisms of formation, genotoxicity, and mutation of guanine oxidation products. *Chem. Res. Toxicol*., **19**, 491–501.
10. Kino,K. and Saito,I. (1998) Product analysis of GG-specific photooxidation of DNA via electron transfer: 2-aminoimidazolone as a major guanine oxidation product. *J. Am. Chem. Soc*., **120**, 7373–7374.
11. Hirakawa,K., Yoshida,M., Oikawa,S. and Kawanishi,S. (2003) Base oxidation at 5′ site of GG sequence in double-stranded DNA induced by UVA in the presence of xanthone analogues: relationship between the DNA-damaging abilities of photosensitizers and their HOMO energies. *Photochem. Photobiol*., **77**, 349–355.
12. Hirakawa,K., Suzuki,H., Oikawa,S. and Kawanishi,S. (2003) Sequence-specific DNA damage induced by ultraviolet A-irradiated folic acid via its photolysis product. *Arch. Biochem. Biophys*., **410**, 261–268.
13. Cadet,J. and Treoule,R. (1978) Comparative study of oxidation of nucleic acid components by hydroxyl radicals, singlet oxygen and superoxide anion radicals. *Photochem. Photobiol*., **28**, 661–667.
14. Douki,T. and Cadet,J. (1996) Peroxynitrite mediated oxidation of purine bases of nucleosides and isolated DNA. *Free Radic. Res*., **24**, 369–380.
15. Luo,W., Muller,J.G., Rachlin,E.M. and Burrows,C.J. (2000) Characterization of spiroiminodihydantoin as a product of one-electron oxidation of 8-oxo-7,8-dihydroguanosine. *Org. Lett*., **2**, 613–616.
16. Niles,J.C., Wishnok,J.S. and Tannenbaum,S.R. (2001) Spiroiminodihydantoin is the major product of the 8-oxo-7,8-dihydroguanosine reaction with peroxynitrite in the presence of thiols and guanosine photooxidation by methylene blue. *Org. Lett*., **3**, 963–966.
17. Luo,W., Muller,J.G., Rachlin,E.M. and Burrows,C.J. (2001) Characterization of hydantoin products from one-electron oxidation of 8- oxo-7,8-dihydroguanosine in a nucleoside model. *Chem. Res. Toxicol*., **14**, 927–938.
18. Ravanat,J.L. and Cadet,J. (1995) Reaction of singlet oxygen with 2′-deoxyguanosine and DNA. Isolation and characterization of the main oxidation products. *Chem. Res. Toxicol*., **8**, 379–388.
19. Cadet,J., Berger,M., Buchko,G.W., Joshi,P.C., Raoul,S. and Ravanat,J.-L. (1997) 2,2-Diamino-4-[3,5-di-*O*-acetyl-2-deoxy-β-D-*erythro*-pentofuranosyl)amino]-5-(2*H*)-oxazolone: a novel and predominant radical oxidation product of 3′,5′-di-*O*-acetyl-2′-deoxyguanosine. *J. Am. Chem. Soc*., **116**, 7403–7404.
20. Helbock,H.J., Beckman,K.B., Shigenaga,M.K., Walter,P.B., Woodall,A.A., Yeo,H.C. and Ames,B.N. (1998) DNA oxidation matters: the HPLC-electrochemical detection assay of 8-oxo-deoxyguanosine and 8-oxo-guanine. *Proc. Natl Acad. Sci. USA*, **95**, 288–293.
21. Malins,D.C. (1996) Free radicals and breast cancer. *Environ. Health Perspect*., **104**, 1140.
22. Dizdaroglu,M., Jaruga,P. and Rodriguez,H. (2001) Measurement of 8-hydroxy-2′-deoxyguanosine in DNA by high-performance liquid chromatography-mass spectrometry: comparison with measurement by gas chromatography-mass spectrometry. *Nucleic Acids Res*., **29**, E12.
23. Gackowski,D., Speina,E., Zielinska,M., Kowalewski,J., Rozalski,R., Siomek,A., Paciorek,T., Tudek,B. and Olinski,R. (2003) Products of oxidative DNA damage and repair as possible biomarkers of susceptibility to lung cancer. *Cancer Res*., **63**, 4899–4902.
24. Collins,A., Cadet,J., Epe,B. and Gedik,C. (1997) Problems in the measurement of 8-oxoguanine in human DNA. Report of a workshop, DNA oxidation, held in Aberdeen, UK, 19–21 January, 1997. *Carcinogenesis*, **18**, 1833–1836.
25. Yanagawa,H., Ogawa,Y. and Ueno,M. (1992) Redox ribonucleosides. Isolation and characterization of 5-hydroxyuridine, 8-hydroxyguanosine, and 8-hydroxyadenosine from Torula yeast RNA. *J. Biol. Chem*., **267**, 13320–13326.
26. Steenken,S. and Jovanovic,S.V. (1997) How easily oxidizable is DNA? One-electron reduction potentials of adenosine and guanosine radicals in aqueous solution *J. Am. Chem. Soc*., **119**, 617–618.
27. Hickerson,R.P., Prat,F., Muller,J.G., Foote,C.S. and Burrows,C.J. (1999) Sequence and stacking dependence of 8-oxoguanine oxidation: comparison of one-electron vs singlet oxygen mechanisms. *J. Am. Chem. Soc*., **121**, 9423–9428.
28. Uppu,R.M., Cueto,R., Squadrito,G.L., Salgo,M.G. and Pryor,W.A. (1996) Competitive reactions of peroxynitrite with 2′-deoxyguanosine and 7,8- dihydro-8-oxo-2′-deoxyguanosine (8-oxodG): relevance to the formation of 8-oxodG in DNA exposed to peroxynitrite. *Free Radic. Biol. Med*., **21**, 407–411.
29. Tretyakova,N.Y., Niles,J.C., Burney,S., Wishnok,J.S. and Tannenbaum,S.R. (1999) Peroxynitrite-induced reactions of synthetic oligonucleotides containing 8-oxoguanine. *Chem. Res. Toxicol*., **12**, 459–466.
30. Nunez,M.E., Rajski,S.R. and Barton,J.K. (2000) Damage to DNA by long-range charge transport. *Methods Enzymol*., **319**, 165–188.
31. Henderson,P.T., Delaney,J.C., Gu,F., Tannenbaum,S.R. and Essigmann,J.M. (2002) Oxidation of 7,8-dihydro-8-oxoguanine affords lesions that are potent sources of replication errors *in vivo*. *Biochemistry*, **41**, 914–921.
32. Duarte,V., Gasparutto,D., Jaquinod,M., Ravanat,J. and Cadet,J. (2001) Repair and mutagenic potential of oxaluric acid, a major product of singlet oxygen-mediated oxidation of 8-oxo-7,8-dihydroguanine. *Chem. Res. Toxicol*., **14**, 46–53.
33. Gasparutto,D., Da Cruz,S., Bourdat,A.G., Jaquinod,M. and Cadet,J. (1999) Synthesis and biochemical properties of cyanuric acid nucleoside- containing DNA oligomers. *Chem. Res. Toxicol*., **12**, 630–638.
34. Henderson,P.T., Neeley,W.L., Delaney,J.C., Gu,F., Niles,J.C., Hah,S.S., Tannenbaum,S.R. and Essigmann,J.M. (2005) Urea lesion formation in DNA as a consequence of 7,8-dihydro-8-oxoguanine oxidation and hydrolysis provides a potent source of point mutations. *Chem. Res. Toxicol*., **18**, 12–18.
35. Henderson,P.T., Delaney,J.C., Muller,J.G., Neeley,W.L., Tannenbaum,S.R., Burrows,C.J. and Essigmann,J.M. (2003) The hydantoin lesions formed from oxidation of 7,8-dihydro-8-oxoguanine are potent sources of replication errors *in vivo*. *Biochemistry*, **42**, 9257–9262.
36. Gasparutto,D., Ravanat,J., Gerot,O. and Cadet,J. (1998) Characterization and chemical stability of photooxidized oligonucleotides that contain 2,2-diamino-4-[(2-deoxy-β-D-*erythro*-pentofuranosyl)amino]-5(2*H*)-oxazolone. *J. Am. Chem. Soc*., **120**, 10283–10286.
37. Douki,T. and Cadet,J. (1999) Modification of DNA bases by photosensitized one-electron oxidation. *Int. J. Radiat. Biol*., **75**, 571–581.
38. Yu,H., Venkatarangan,L., Wishnok,J.S. and Tannenbaum,S.R. (2005) Quantitation of four guanine oxidation products from reaction of DNA with varying doses of peroxynitrite. *Chem. Res. Toxicol*., **18**, 1849–1857.
39. Misiaszek,R., Crean,C., Joffe,A., Geacintov,N.E. and Shafirovich,V. (2004) Oxidative DNA damage associated with combination of guanine and superoxide radicals and repair mechanisms *via* radical trapping. *J. Biol. Chem*., **279**, 32106–32115.
40. Vialas,C., Pratviel,G.C.C. and Meunier,B. (1998) Efficient oxidation of 2′-deoxyguanosine by Mn-TMPyP/KHSO5 to imidazolone dIz without formation of 8-oxo-dG. *J. Am. Chem. Soc*., **120**, 11548–11553.
41. Tretyakova,N.Y., Wishnok,J.S. and Tannenbaum,S.R. (2000) Peroxynitrite-induced secondary oxidative lesions at guanine nucleobases: chemical stability and recognition by the Fpg DNA repair enzyme. *Chem. Res. Toxicol*., **13**, 658–664.
42. Burrows,C.J. and Muller,J.G. (1998) Oxidative nucleobase modifications leading to strand scission. *Chem. Rev*., **98**, 1109–1152.
43. Duarte,V., Gasparutto,D., Jaquinod,M. and Cadet,J. (2000) *In vitro* DNA synthesis opposite oxazolone and repair of this DNA damage using modified oligonucleotides. *Nucleic Acids Res*., **28**, 1555–1563.
44. Gallaher,D.D., Csallany,A.S., Shoeman,D.W. and Olson,J.M. (1993) Diabetes increases excretion of urinary malonaldehyde conjugates in rats. *Lipids*, **28**, 663–666.
45. Kim,S.S., Gallaher,D.D. and Csallany,A.S. (2000) Vitamin E and probucol reduce urinary lipophilic aldehydes and renal enlargement in streptozotocin-induced diabetic rats. *Lipids*, **35**, 1225–1237.
46. Kasai,H. and Nishimura,S. (1984) Hydroxylation of deoxyguanosine at the C-8 position by ascorbic acid and other reducing agents. *Nucleic Acids Res*., **12**, 2137–2145.
47. Frelon,S., Douki,T., Ravanat,J.L., Pouget,J.P., Tornabene,C. and Cadet,J. (2000) High-performance liquid chromatography—tandem mass spectrometry measurement of radiation-induced base damage to isolated and cellular DNA. *Chem. Res. Toxicol*., **13**, 1002–1010.

48. Hofer,T. and Möller,L. (2002) Optimization of the workup procedure for the analysis of 8-oxo-7,8- dihydro-2′-deoxyguanosine with electrochemical detection. *Chem. Res. Toxicol*., **15**, 426–432.
49. Crain,P.F. (1990) Preparation and enzymatic hydrolysis of DNA and RNA for mass spectrometry. *Methods Enzymol*., **193**, 782–790.
50. Dong,M., Wang,C., Deen,W.M. and Dedon,P.C. (2003) Absence of 2′-deoxyoxanosine and presence of abasic sites in DNA exposed to nitric oxide at controlled physiological concentrations. *Chem. Res. Toxicol*., **16**, 1044–1055.
51. Buchko,G.W., Cadet,J., Ravanat,J.L. and Labataille,P. (1993) Isolation and characterization of a new product produced by ionizing irradiation and type I photosensitization of 2′-deoxyguanosine in oxygen-saturated aqueous solution: (2*S*)-2,5′-anhydro-1-(2′-deoxy-β-D-erythro-pentofuranosyl)-5-guanidinylidene-2-hydroxy-4-oxoimidazolidine. *Int. J. Radiat. Biol*., **63**, 669–676.
52. Chaudhary,A.K., Reddy,G.R., Blair,I.A. and Marnett,L.J. (1996) Characterization of an N^6-oxopropenyl-2′-deoxyadenosine adduct in malondialdehyde-modified DNA using liquid chromatography/electrospray ionization tandem mass spectrometry. *Carcinogenesis*, **17**, 1167–1170.
53. Ravanat,J.L., Duretz,B., Guiller,A., Douki,T. and Cadet,J. (1998) Isotope dilution high-performance liquid chromatography-electrospray tandem mass spectrometry assay for the measurement of 8-oxo-7,8-dihydro-2′-deoxyguanosine in biological samples. *J. Chromatogr. B Biomed. Sci. Appl*., **715**, 349–356.
54. Churchwell,M.I., Beland,F.A. and Doerge,D.R. (2002) Quantification of multiple DNA adducts formed through oxidative stress using liquid chromatography and electrospray tandem mass spectrometry. *Chem. Res. Toxicol*., **15**, 1295–1301.
55. Ueno,Y., Kizaki,M., Nakagiri,R., Kamiya,T., Sumi,H. and Osawa,T. (2002) Dietary glutathione protects rats from diabetic nephropathy and neuropathy. *J. Nutr*., **132**, 897–900.
56. Kino,K. and Sugiyama,H. (2001) Possible cause of GC→CG transversion mutation by guanine oxidation product, imidazolone. *Chem. Biol*., **8**, 369–378.